Hindawi
Journal of Nanomaterials
Volume 2022, Article ID 6596028, 11 pages
https://doi.org/10.1155/2022/6596028

Research Article

An Experimental Study of ZrO_2-CeO_2 Hybrid Nanofluid and Response Surface Methodology for the Prediction of Heat Transfer Performance: The New Correlations

R. Vidhya,[1] T. Balakrishnan,[2] B. Suresh Kumar,[3] R. Palanisamy,[4] Hitesh Panchal,[5] Luis Angulo-Cabanillas,[6] Saboor Shaik,[7] B. Saleh,[8] and Ibrahim M. Alarifi[9]

[1]*PG and Research Department of Physics, Bishop Heber College (Autonomous), (Affiliated to Bharathidasan University), Tiruchirappalli 620017, Tamilnadu, India*
[2]*Crystal Growth Laboratory, PG and Research Department of Physics, Thanthai Periyar Government Arts and Science College (Autonomous), (Affiliated to Bharathidasan University), Tiruchirappalli 620023, Tamilnadu, India*
[3]*Department of Mechanical Engineering, K.Ramakrishnan College of Technology, Samayapuram, Tiruchirappalli, Tamil Nadu 621112, India*
[4]*Dept. of EEE, SRM Institute of Science and Technology, Kattankulathur, Chennai 603203, India*
[5]*Mechanical Engineering Department, Government Engineering College Patan, Gujarat, India*
[6]*Universidad Nacional Santiago Antunez de Mayolo, Huaraz, Peru*
[7]*School of Mechanical Engineering, Vellore Institute of Technology, Vellore, 632014 Tamil Nadu, India*
[8]*Mechanical Engineering Department, College of Engineering, Taif University, P.O. Box 11099, Taif 21944, Saudi Arabia*
[9]*Department of Mechanical and Industrial Engineering, College of Engineering, Majmaah University, Al-Majmaah, Riyadh 11952, Saudi Arabia*

Correspondence should be addressed to T. Balakrishnan; balacrystalgrowth@gmail.com
and Ibrahim M. Alarifi; i.alarifi@mu.edu.sa

Received 22 March 2022; Accepted 19 May 2022; Published 20 June 2022

Academic Editor: Ana Espinosa

This article experimentally and statistically reports the convective heat transfer performance of a cylindrical mesh-type heat pipe apparatus filled with ZrO_2-CeO_2/water-ethylene glycol nanofluids. In this regard, ZrO_2-CeO_2 nanoparticles were synthesized and characterized through the Scanning Electron Microscope and Powder X-ray diffraction methods followed by the preparation of hybrid ZrO_2-CeO_2 nanofluids of various concentrations ranging from 0.025 to 0.1%. The heat transfer features of a tubular heat pipe with a mixture of the ZrO_2-CeO_2 nanofluid were evaluated. A 5.33% decrease in thermal resistance value and a 41.16% increase in heat transfer ability with increased power input were observed. The potent regression models were proposed to estimate heat transfer features of the heat pipe. The ANOVA statistical method has been employed to determine the *P* value and the *F* value of the models towards enhancing the reliability and accuracy of the developed models. The outcome revealed that the proposed models are reliable and have the best fit with the experimental data for 30–60 W power. The correlations' results were validated against the experimental data and showed high accuracy. Moreover, the accuracy of the developed models was ensured through *R*-squared and adjusted *R*-squared values.

1. Introduction

Choi [1] introduced the dispersion of 1–100 nm particles into the base fluid, called the nanofluid. These nanofluids have distinct thermal and hydrodynamic properties [2–4]. Nanofluids reduce energy consumption in the industries by decreasing the heat losses within the heat exchangers. Therefore, nanofluids attracted the attention of many researchers in the latest years because of their enhanced hydrodynamic and heat exchanging phenomenon. A heat

pipe device is one of the modest heat exchangers that work on the capillary action and phase change principle. It transfers a massive quantity of heat [5]. The nanofluid is a potential fluid with a high thermal conductivity and stability compared to other fluids like water, EG, oils, and microfluids [6, 7]. Hence, nanofluids are used as heat transfer liquids in various heat exchanging systems, such as computers, solar collectors, cooling electronic devices, and microelectronics [8].

Chien et al. [9] first analyzed the heat pipe efficiency using nanofluids, followed by many experimental studies to estimate the heat transfer proficiency on various heat pipes [10–14]. Solomon et al. [15] determined that adding 0.1% Cu/W nanoliquid increased the heat transferring ability by about 20%. Akbari and Saidi [16] examined the pulsating type heat pipe's thermal performance and flow regimes using graphene and titania nanofluids, reporting that the nanofluid improved thermal performance by 70% flow regimes at 70 W. A two-phase thermosyphon's heat transfer behavior charged with Ag/W nanofluid had shown the augmented result by applying a strong magnetic field [17]. Ghanbarpour et al. [18] performed experimentation with a silicon carbide nanofluid in a tubular heat pipe and originated the thermal resistivity value of 30% for 1.0% particle weight concentrations. Zeinali Heris et al. [19, 20] tested the heat transfer proficiency of the thermosyphon and car radiator with oxidized CNT/water and CuO/EG-W nanofluids. It is noticed from the literature that high heat transfer appearances with nanoparticles in aqueous EG deliver significant outcomes over the traditional base liquids [21–24]. Keshavarz Moraveji and Razvarz [25] found that the sintered wick pipe's heat transferring characteristics were improved when using an alumina nanofluid, especially at 3% particle concentration. Noie et al. [26] analyzed the alumina nanofluids in the thermosyphon, resulting in enhanced system efficiency with respect to power and particle weight concentration. Using TiO_2-SiO_2/W-EG hybrid nanofluids, Nabil et al. [21] observed 22.8% enrichment in thermal conductivity at 3% weight concentration as the weight concentration increases. Akilu et al. [22] achieved the augmented thermophysical properties 1.15 times and 26.9% higher with the SiO_2–G/EG nanofluid than the base fluid.

Ghalambaz et al. [27] demonstrated the increment in the thermal performance of the double-pipe heat exchanger using alumina nanoparticles. They have also observed the enhancement in the Nusselt number for alumina nanoparticles and twisted tape inserts with the help of a two-phase nanofluid model. Due to the enhanced thermal features of nanofluids, nanocoolants have been utilized to transfer a large quantity of heat more efficiently in car radiators [28, 29]. A great part of the literature is devoted to the investigation of nanofluid-based nonconcentrating collectors. The analysis of nanofluids based nonconcentrating solar systems especially in solar collectors has been found to increase thermal efficiency [30–32]. The researchers also recommended that nanofluids in mechanical operations such as cutting and drilling reduce the production of excessive heat during the machining operations [33, 34]. Nanofluids hold great significance in biomedical industries such as antibacterial cases, cryopreservation, dressing of wounds, and drug delivery also [35, 36].

Based on the above literature, additional investigation is required on the potential applications of the hybrid nanofluids as the working medium in heat pipes. We chose zirconia nanofluids because they have significant thermophysical features and have recently been used for various heat transfer applications [37–39]. Ceria nanofluids also exhibited improved efficiency in flat-type solar collectors [40]. Mary et al. [41] evaluated the improved transport properties with cerium oxide/ethylene glycol nanofluids. However, the thermal transfer performance of ZrO_2-CeO_2 nanofluids dispersed in the W-EG fluid in a screen mesh heat pipe has not been examined so far. In addition, it is expected that anomalous thermal features can be accomplished by applying the heat transfer of a hybrid ZrO_2-CeO_2 fluid with a wick-structured heat pipe. Therefore, in the current research, an investigation is conducted for estimating the thermal resistance attributes of the tubular heat pipe filled with a ZrO_2-CeO_2 nanofluid for the first time.

Recently, many researchers experimentally and statistically focused on investigating the thermophysical properties of nanofluids and their heat transfer behavior [42–45]. Response surface methodology (RSM) is a more suitable technique than the genetic algorithms (GA) and artificial neural networks (ANN) to obtain all information among input variables from minimum experimental data [46]. Moreover, RSM provides acceptable precision compared to GA and ANN algorithms [47, 48].

The present study analyzes the experimental and statistical thermal resistance and heat transfer coefficient of a tubular heat pipe filled with ZrO_2-CeO_2/W-EG nanofluids. RSM with the ANOVA technique was engaged to examine the influence of input variables on thermal resistance and heat transfer coefficient properties. In addition, two new regression correlations on considered responses were proposed with the regression analysis.

2. Methodology

The first part of this section explains the nanofluid preparation, and the second one deals with the experimental arrangement used for measurements.

2.1. Synthesis and Characterization of ZrO_2-CeO_2 Nanoparticles. In this ZrO_2 (zirconia) nanoparticle preparation, zirconium oxychloride was used as the precursor solution via the sol-gel method. 0.6 M of aqueous ammonia solution was slowly added to the precursor solution (0.7 M) for 30 minutes under constant stirring. Then, a slurry gel with white color was procured. Finally, it was calcinated for five hours at the temperature of 750°C in a muffle furnace to obtain the zirconia nanoparticles.

In the CeO_2 (ceria) nanopowder synthesis, an aqueous ammonia solution (0.8 M) was slowly added to the ceric nitrate solution (0.8 M) for 30 minutes at ambient temperature under constant stirring. The colloidal suspension was heated up to 100°C overnight and then washed thrice with EG and distilled water to remove the contaminants. The

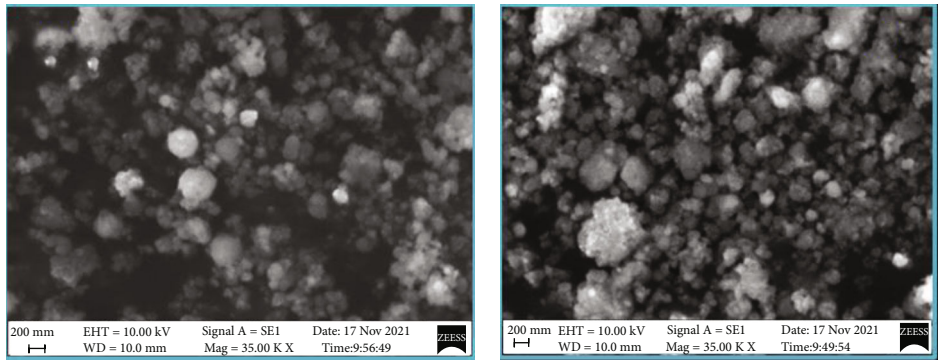

(a) (b)

FIGURE 1: SEM picture of (a) ZrO_2 and (b) CeO_2 nanoparticles.

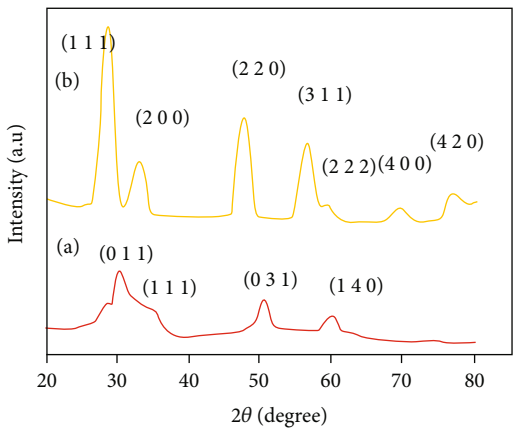

FIGURE 2: Powder X-ray diffraction structure of (a) zirconia and (b) ceria samples.

precipitate obtained was calcinated at the temperature of 650°C using a muffle furnace for four hours and finally powdered using a mortar and pestle. The pale yellow CeO_2 powder was stored in an airtight vial for further investigation.

The structural characterizations of synthesized ZrO_2 and CeO_2 nanoparticles were carried out through the Powder X-ray diffraction (PXRD) method and surface morphology through a Scanning Electron Microscope (SEM). SEM analysis is used to identify the surface structure of the nanoparticles. The SEM pictures of zirconia and ceria nanoparticles recorded with the JEOL, JSM 6390 instrument, are depicted in Figures 1(a) and 1(b), correspondingly. SEM pictures show that both ZrO_2 and CeO_2 nanoparticles have a spherical shape, white color, and slight agglomeration with the neighboring nanoparticles. ImageJ software is used to determine the nanoparticle size, and it was found as 80 nm for ZrO_2 and 70 nm for CeO_2 particles.

X-ray diffraction results of zirconia and ceria nanoparticles are displayed in Figures 2(a) and 2(b) with the help of the X'pert Pro instrument. The scattering angle (2θ) identification procedure has been tuned between 80° and 10° at 0.05° intervals. It clearly shows that the strong peaks at the scattering angle of 30.10°, 35.22°, 50.42°, and 60.04° correspond to (0 1 1), (1 1 1), (0 3 1), and (1 4 0), respectively, well matched with the JCPDS card no: 83–0810. These planes reveal the formation of the orthorhombic structure of ZrO_2 nanoparticles. The XRD pattern shows a high intense (0 1 1) positioning peak, denoting a high crystallinity of the synthesized sample. Similarly, the diffraction peaks in Figure 2(b) at 28.53°, 33.07°, 47.56°, 56.32°, 59.15°, 69.4°, and 79.04° scattering angles are associated with (1 1 1), (2 0 0), (2 2 0), (3 1 1), (2 2 2), (4 0 0), and (4 2 0) planes, respectively. The CeO_2 particles with a cubic structure have been observed from XRD results, which agree with JCPDS: 65-2975. The average size of ZrO_2 and CeO_2 crystallites (D) is measured using the following Debye–Scherrer equation:

$$D = \frac{K\lambda}{\beta \cos\theta}, \tag{1}$$

where K stands for the constant shape factor (1.9), β states Full Width at Half Maximum, λ is the wavelength (1.5405 Å) of the X-ray source, and θ denotes the diffraction angle. From the XRD results, ZrO_2 and CeO_2 crystallites' average size was found as 2.2 nm and 7.07 nm, respectively. Since the crystallites are very small in dimension, they will render a superior efficiency in heat transfer characteristics [49].

2.2. Synthesis of ZrO_2-CeO_2 Nanofluids. The synthesis of ZrO_2-CeO_2 hybrid nanofluids has been made through a two-step approach with the prepared ZrO_2 and CeO_2 nanoparticles. ZrO_2 and CeO_2 nanoparticles (50 : 50) were suspended in the W-EG fluid (60/40%) in the first step. A 60 : 40 proportion of the W-EG mixture exhibited superior and significant performance with regard to the thermal characteristics of nanofluid production [21–24]. A small amount (2.5 g) of cetyltrimethylammonium bromide surfactant (CTAB) was added to the above combination with the preparation of the nanofluids of all particle weight concentrations to attain the stability of the fluids [25, 26]. An ultrasonicator (50 Hz, 170 V AC-270 V AC, 50 Hz) was utilized to prepare all volume concentrations of nanoparticles to avoid nanoparticle settlement in the base fluid [22]. Thus, hybrid ZrO_2-CeO_2 nanofluids for various volume

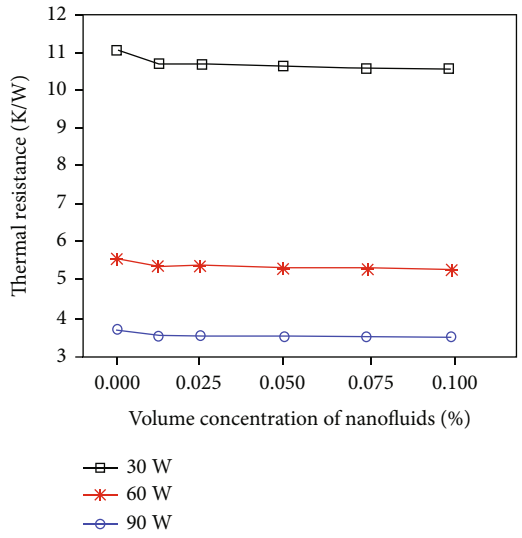

Figure 3: Thermal resistance variation of ZrO_2-CeO_2 nanofluids with respect to volume concentrations and at different heat power input values.

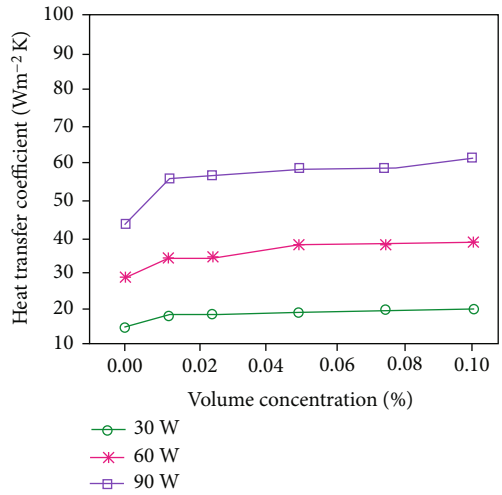

Figure 4: Heat power input and volume concentration effects on the heat transfer coefficient by using ZrO_2-CeO_2 nanofluids.

Table 1: Heat transfer coefficient comparative study on nanofluids at 0.1% volume concentration.

Nanofluid	Base fluid proportion	Increase % of heat transfer coefficient		
		30 W	60 W	90 W
ZrO_2/W-EG	W-60% EG-40%	25.11	26.18	27.19
CeO_2/W-EG	W-60% EG-40%	26.83	27.13	36.18
ZrO_2-CeO_2/W-EG	W-60% EG-40%	27.19	28.11	38.16

concentrations (φ) of a range from 0.0125 to 0.1% were made in room temperature using the following equation:

$$\phi = \frac{w_{np}/\rho_{np}}{w_{np}/\rho_{np} + w_{bf}/\rho_{bf}} * 100, \quad (2)$$

where w_{np} and ρ_{np} indicate the w_{np} mass and density of ZrO_2 and CeO_2 particles, respectively, and w_{bf} and ρ_{np} represent the mass and density of the suspension (W-EG), respectively.

2.3. Experimental Apparatus and Process. The schematic and working principle of a cylindrical heat pipe device fabricated for inspecting heat transfer operation was reported earlier in our previous work [50]. The six various particle weight concentrations (0%, 0.0125%, 0.025%, 0.05%, 0.075%, and 0.1%) of ZrO_2-CeO_2 hybrid nanofluids were utilized for experimentation with the heat pipe. The experiment was conducted initially with a base fluid, followed by ZrO_2, CeO_2, and ZrO_2-CeO_2 hybrid nanofluids. The position of the heat pipe was set up at 45° orientation since the efficiency of the heat pipe is enriched at this position [51, 52]. The heat transfer rates were calculated for the three heat power inputs in the range of 30–90 W. The following equations (3) and (4) are utilized to determine the heat pipe's heat transfer characteristics.

$$\text{Thermal resistance } (R) = \frac{T_e - T_c}{Q}, \quad (3)$$

$$\text{Heat transfer coefficient } (h) = \frac{Q}{A(T_e - T_c)}, \quad (4)$$

where T_e and T_c stand for the temperature of the evaporator and condenser sections, respectively. $Q = I * V$ represents the input heat power and $A = \pi dl$ (d: internal diameter; l: overall length of tubular heat pipe device).

Uncertainty of all the quantities used in this heat pipe experimentation was estimated using standard procedure [53]. The current, area, and voltage uncertainty values were found as ±0.2, ±0.25%, and ±0.25%, respectively. The maximum uncertainty value of power (Q), thermal resistivity (R), and heat transfer coefficient (h) was determined as ±2.76%, ± 2.76%, and ± 2.91%, respectively, using the following equations:

$$\frac{\Delta Q}{Q} = \sqrt{\left(\frac{\Delta V}{V}\right)^2 + \left(\frac{\Delta I}{I}\right)^2} = \pm 2.76\%, \quad (5)$$

$$\frac{\Delta R}{R} = \sqrt{\left(\frac{\Delta Q}{Q}\right)^2 + \left(\frac{\Delta(\Delta T_{e/c})}{\Delta T_{e/c}}\right)^2} = \pm 2.76\%, \quad (6)$$

$$\frac{\Delta h}{h} = \sqrt{\left(\frac{\Delta Q}{Q}\right)^2 + \left(\frac{\Delta A_{e/c}}{A_{e/c}}\right)^2 + \left(\frac{\Delta(\Delta T_{e/c})}{\Delta T_{e/c}}\right)^2} = \pm 2.85\%. \quad (7)$$

Table 2: Developed regression model outline.

Quadratic model	Standard deviation	R-squared	Adj. R-squared	Predicted R-squared	Adequate precision	
Thermal resistance	0.063	0.9997	0.9996	0.99923	203.273	Suggested
Heat transfer coefficient	2.26	0.9859	0.9801	0.9622	34.722	Suggested

Table 3: Thermal resistance and heat transfer coefficient variance analysis.

Source	Sum of squares	Degrees of freedom	Mean square	F value	P value prob > F
Thermal resistance					
Model	165.42	5	33.08	8249.02	<0.0001
A: power	147.69	1	147.69	36824.82	<0.0001
B: volume concentration	0.12	1	0.12	29.90	0.0001
AB	0.023	1	0.023	5.81	0.0329
A^2	12.20	1	12.20	3043.05	<0.0001
B^2	0.043	1	0.043	10.64	0.0068
Residual	0.048	12	4.011E-003		
Total	165.4717				
Heat transfer coefficient					
Model	4289.64	5	857.93	168.13	< 0.0001
A: power	4050.35	1	4050.35	793.78	< 0.0001
B: volume concentration	131.34	1	131.34	25.74	0.0003
AB	19.35	1	19.35	3.79	0.0752
A^2	12.19	1	12.19	2.39	0.1482
B^2	45.13	1	45.13	8.84	0.0116
Residual	61.23	12	5.10		
Total	4350.87	17			

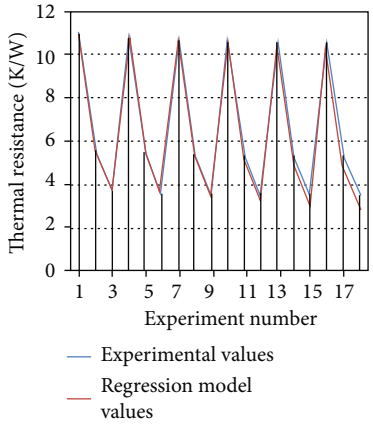

Figure 5: Validation of the RSM model of thermal resistance against the empirical data.

3. Response Surface Methodology (RSM)

RSM remains a powerful method to recognize the impacts of input factors on the measured outcomes coupled with the mathematical and statistical methods [25]. In general, the RSM approach is widely utilized in engineering, especially in nanofluids' heat and mass transfer applications [54–56]. This study develops a regression model using the experimental data acquired from the heat pipe to assess the response parameters combined with RSM. Variance analysis denotes such substantial values amongst the various input factors and responses. To evaluate the consistency between recommended RSM models and measured data, it is important to inspect the statistical elements, i.e., R-squared (R^2), adjacent R-squared (Adj. R^2), probability value (P value), and Fisher's test (F test) value.

4. Results and Discussion

4.1. Experimental Results of the Heat Transfer Properties of Heat Pipe. The volume concentration of nanofluids, heat power input, and positioning of the heat pipe are the significant factors inducing the features of heat transfer. To assess such factors, it is necessary to examine heat transfer characteristics. Figure 3 represents the values of thermal resistance against different volume concentrations at 30, 60, and 90 W heat powers. As evident, adding ZrO_2 and CeO_2 nanoparticles into W-EG diminishes the thermal resistance values intensely. When the surface wettability rises, fluid resistance decreases due to the settlement of ZrO_2 and CeO_2 nanoparticles on the wick structure of the evaporation section.

Table 4: Validation of proposed regression models with experimental data.

Exp. no.	Volume concentration (%)	Power (W)	Experimental values of R (K/W)	Regression model values of R (K/W)	Experimental values of h (W/m^{2}K)	Regression model values of h (W/m^{2}K)	% of deviation in R	% of deviation in h
1	0	30	11.06	10.92984	14.8816	14.49894	1.17689	2.571405
2	0	60	5.57	5.557304	28.5514	29.60766	0.227935	-3.69966
3	0	90	3.71	3.678284	43.3209	48.20766	0.854879	-11.2803
4	0.0125	30	10.71	10.79815	18.1475	16.81907	-0.8231	7.320428
5	0.0125	60	5.41	5.409967	33.9082	32.37916	0.000614	4.509315
6	0.0125	90	3.56	3.515292	55.5937	51.43053	1.255852	7.488492
7	0.025	30	10.7	10.68239	18.223	18.62172	0.164613	-2.18798
8	0.025	60	5.4	5.278544	34.2393	34.63318	2.249182	-1.15031
9	0.025	90	3.55	3.368214	56.3079	54.13592	5.120734	3.857366
10	0.05	30	10.64	10.4986	18.9724	20.67459	1.328992	-8.97169
11	0.05	60	5.33	5.063443	37.299	37.58878	5.001075	-0.7769
12	0.05	90	3.54	3.121802	57.54	57.99426	11.8135	-0.78939
13	0.075	30	10.58	10.37846	19.7416	20.65753	1.904892	-4.63966
14	0.075	60	5.33	4.912	37.6192	38.47447	7.842408	-2.27357
15	0.075	90	3.53	2.939049	58.696	59.78268	16.74082	-1.8514
16	0.1	30	10.57	10.32199	19.8759	18.57056	2.346377	6.56737
17	0.1	60	5.31	4.824215	38.4441	37.29023	9.148495	3.001538
18	0.1	90	3.51	2.819954	61.153	59.50118	19.65943	2.701152
						Mean	4.778533	0.022009

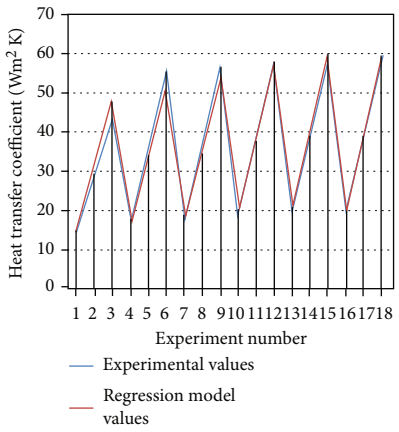

Figure 6: Validation of the RSM model of heat transfer coefficient against the empirical data.

Similarly, thermal resistance decreases with the rise of heat power input. The minimum resistance value of 3.51 K/W is detected for 0.1% concentration at the heat input of 90 W, which shows a 4.8% reduction in the thermal resistance value over the base fluid. This demonstrates the augmented efficiency of heat pipes using ZrO_2-CeO_2 hybrid nanofluids.

Figure 4 depicts the heat transfer coefficient values as a function of volume concentrations and heat input. The maximum and minimum heat transfer coefficient values are 14.88 and 61.15 W/m^{2}K for 0.0125% and 0.1% particle weight concentrations. At 90 W, a supreme enhancement is observed that is 41.16% more than the base fluid mixture. This enhancement (41.16%) is better than the W-EG fluid mixture and better than other reported nanofluids [30]. Table 1 represents the heat transfer value comparison between hybrid ZrO_2-CeO_2 nanofluids and other fluids. The maximum of 38.16% rise in heat transfer coefficient value is obtained for the 90 W input heat power at 0.1% volume concentration over the single-component fluids (0% concentration) [57–61].

4.2. RSM Approach with ANOVA Technique. In the response surface method, the empirical data obtained through the experimentation are fixed as input variables. For analyzing the empirical data, the Design-Expert software is utilized in this study. RSM with regression analysis would be the best-suited combination to straightforward predict the output parameters [62–67]. Therefore, the present research work has utilized the RSM method with statistical ANOVA. Table 2 denotes the model summary of the suggested quadratic models.

In this work, the quadratic model is the suggested model in both R and h, and the developed models also have good predictability because the quadratic models have a significantly closer R-squared value as 1. As it is clear from Table 2, R-squared values of the resistance and heat transfer coefficient are 0.9997 and 0.9859, respectively, showing the developed models' precision. R-squared values indicate that 99% of the experimental data confirm the responses forecasted by both models. The matching of "predicted R-squared" values 0.9622 and 0.9992 with "Adj. R-squared" values 0.9801 and 0.9996, respectively, is almost good with each other. "Adequate precision" is described as the ratio

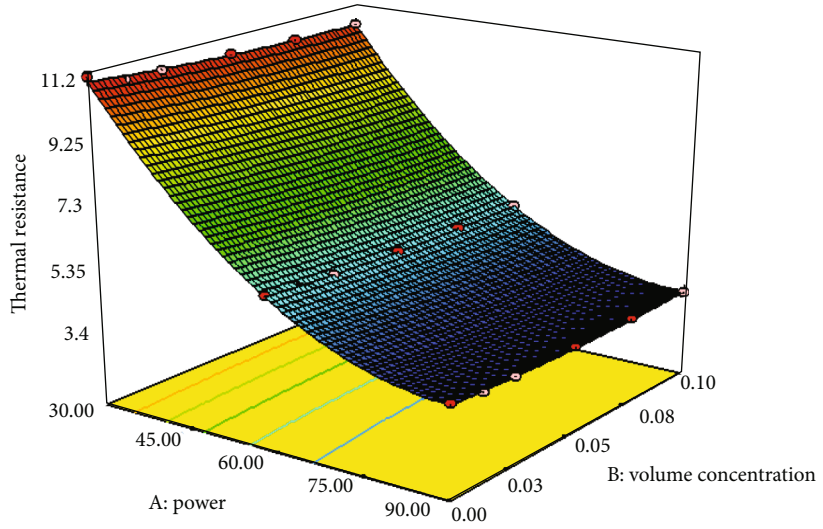

Figure 7: Response surface chart of thermal resistance. Red dots are the experimental data, while the surface is the proposed model results.

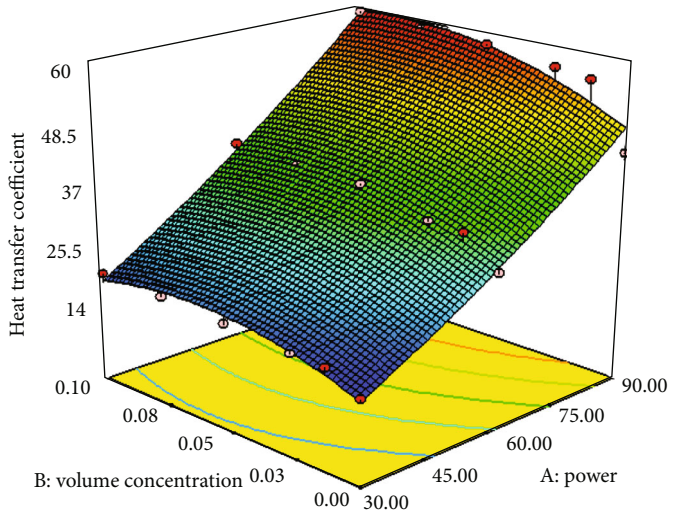

Figure 8: Response surface chart of heat transfer coefficient. Red dots are the experimental data, while the surface is the proposed model results.

of signal and noise factors that should be greater than 4 [68–72]. According to Table 2, the ratio of both models is 203.273 and 34.722, indicating satisfactory signals.

Table 3 summarizes the variance analysis responses of the thermal resistance quadratic model and heat transfer coefficient quadratic model. It is identified that the models are significant as the F value is 8249.02 and 168.13 for the thermal resistance and heat transfer coefficient, respectively. The F values of 8249.02 and 168.13 denote the significance of the models. If "Prob > F" falls below 0.05 and above 0.1, then the model terms are supposed to be substantial terms. All responses acquired with these models are closer to standard values representing the models' high accuracy and consistency with the experimental responses [73–76].

4.3. Developing Mathematical Models Using Regression Analysis. Regression models are formulated based on ANOVA table output. Experimental results of thermal resistance (R) and heat transfer coefficient (h) values were compared to the developed regression models in order to establish a correlation. The obtained third-order polynomial models depict the interactions between the input parameters volume concentration (A) and power (B). The R and h quadratic models are correlated by the following equations.

$$R = 19.79588 - 0.35376 * P - 9.91874 * \phi - 0.041747 * \phi P + 50.92669 * \phi^2 + 1.94084E - 003 * P^2, \quad (8)$$

$$h = 2.88150 + 191.95901 * \phi + 0.32906 * P + 1.20365 * \phi P\text{-}1655.93390 * \phi^2 + 1.93960E - 003 * P^2. \quad (9)$$

4.4. RSM Model Validation with the Empirical Data. The assessment of error between the proposed model values and the experimental data of ZrO_2-CeO_2 hybrid nanofluids are essential to estimate the accuracy of the RSM model. The validation of empirical and predicted RSM model results is displayed in Figures 5 and 6. Table 4 lists the validation results of the RSM regression model and experimental values with the percentage of deviation. The mean originality of models from the experimental data is estimated to be 4.8% and -0.02% for thermal resistance and heat transfer coefficient, respectively, which is minor. The validated percentage of deviation assured the high predictability of both of the proposed models. These low margins of deviation prove that the proposed RSM models have higher predictability on the responses of heat pipes using ZrO_2-CeO_2/W-EG hybrid nanofluids.

The 3-D graphs of a response surface for heat transfer experimental measurements are shown in Figures 7 and 8. It can be seen that the surface formed with the new regression correlations and the collected data from the experimental setup on R and h values (of ZrO_2-CeO_2 hybrid nanofluids) are closely taking place, demonstrating an excellent agreement of the proposed models with the experimental data. These results recommend that the RSM correlations accurately evaluate heat transfer characteristics of heat pipes that use ZrO_2-CeO_2/W-EG hybrid nanofluids.

5. Conclusion

The present study examined the synthesis, structural, and surface characterizations of ZrO_2 and CeO_2 nanoparticles produced by sol-gel and coprecipitation methods. The thermal transfer behavior on a cylindrical mesh-type heat pipe using ZrO_2-CeO_2 nanoparticles in W-EG suspension was investigated. Further, the RSM technique was employed to design experiments, model process variables, and validate the results. The following major conclusions have been drawn through this examination.

The average sizes of ZrO_2 and CeO_2 nanoparticles were found to be 80 nm and 70 nm, respectively, and the shapes of the particles were found to be spherical for both samples through the SEM studies. From the XRD pattern of ZrO_2 and CeO_2 samples, the crystallite sizes were determined to be 2.2 nm and 7.07 nm, respectively.

A statistical approach using a response surface methodology combined with ANOVA was engaged to predict the heat transfer attributes (R: thermal resistance; h: heat transfer coefficient) of the heat pipe of ZrO_2-CeO_2/W-EG hybrid nanofluids. A cylindrical heat pipe experiment has been performed using ZrO_2-CeO_2/W-EG hybrid nanofluids at different particle weight concentrations for various temperatures. It showed 5.33% and 41.16% enhancement in thermal resistance and heat transfer coefficient, respectively, over the base fluid mixture. The developed regression models for R and h can predict the heat transfer performance with the average deviation of 4.8% and 0.02% over the experimental data at a heat input power in the range of 30–90 W and volume concentrations in the range of 0.0125–0.1%. The validation of both the modeling results is well matched with the experimental data. In addition, the values of R^2 (0.9997 and 0.9859) and Adj.R^2 (0.9801 and 0.9996) demonstrated the accuracy of the proposed RSM models vs. the experimental data. Moreover, the ANOVA technique showed significant results with the developed correlations. Hence, it is emphasized that these proposed mathematical models can be utilized for prediction of heat transfer coefficient and thermal resistivity of ZrO_2-CeO_2/W-EG hybrid nanofluids with a cylindrical screen mesh heat pipe. it has been concluded that the hybrid ZrO_2-CeO_2/W-EG nanofluid has superior potential for thermal performance and is highly suitable for heat transfer applications in various heat exchanging systems. In this work, major investigations had been carried out on the most commonly used cylindrical-shaped screen mesh heat pipe in industrial applications due to simplicity in construction, handling, filling, and refilling of the working fluid. Future research direction may focus on the study on variation of heat pipe performance using different types of wick structure, different cross-sections of heat pipe such as square and triangle, various hybrid nanofluids, etc. A heat pipe with enhanced thermal performance has major applications in the field of refrigeration and air conditioning system, satellite equipment, electronic component cooling, automobile radiator, high power LED cooling, microreactors, phase change materials (PCM), etc. These are some of the probable directions on which work can be performed on hybrid nanofluids by researchers in the future for dissemination of their use in different applications.

Data Availability

Data are available upon journal request.

Conflicts of Interest

The authors declare that they have no conflicts of interest.

Acknowledgments

The author B. Saleh is grateful to the Taif University Researchers Supporting Project number (TURSP-2020/49), Taif University, Taif, Saudi Arabia, for the financial support.

References

[1] S. U. S. Choi, *Enhancing thermal conductivity of fluids with nanoparticles developments and applications of non-Newtonian flows*, D. A. Siginer and H. P. Wang, Eds., vol. 66, ASME, New York, 1995.

[2] R. K. Bumataria, N. K. Chavda, and H. Panchal, "Current research aspects in mono and hybrid nanofluid based heat pipe technologies," *Heliyon*, vol. 5, no. 5, p. e0162, 2019.

[3] R. Walvekar, Y. Y. Chen, R. Saputra et al., "Deep eutectic solvents-based CNT nanofluid - a potential alternative to conventional heat transfer fluids," *Journal of the Taiwan Institute of Chemical Engineers*, vol. 128, pp. 314–326, 2021.

[4] E. Medhat, E. A. El, H. A.-E. B. Shenawy, M. M. Shams, and H. Panchal, "A comprehensive review on the effects of diesel/biofuel blends with nanofluid additives on compression

ignition engine by response surface methodology," *Energy Conversion and Management*, vol. 14, p. 100177, 2022.

[5] H. S. Lee, *Thermal Design: Heat Sinks, Thermoelectrics, Heat Pipes, Compact Heat Exchangers, and Solar Cells*, Wiley, Newyork, 2010.

[6] M. Rahimi-Gorji, O. Pourmehran, M. Hatami, and D. D. Ganji, "Statistical optimization of microchannel heat sink (MCHS) geometry coolThe European Physical Journal Plus," vol. 130, no. 2, pp. 1–21, 2015.

[7] G. Żyła, "Thermophysical properties of ethylene glycol based yttrium aluminum garnet ($Y_3Al_5O_{12}$-EG) nanofluids," *International Journal of Heat and Mass Transfer*, vol. 92, pp. 751–756, 2016.

[8] C. Yıldız, M. Arıcı, and H. Karabay, "Comparison of a theoretical and experimental thermal conductivity model on the heat transfer performance of Al_2O_3-SiO_2/water hybrid-nanofluid," *International Journal of Heat and Mass Transfer*, vol. 140, pp. 598–605, 2019.

[9] H.-T. Chien, C.-I. Tsai, P.-H. Chen, and P.-Y. Chen, "Improvement on thermal performance of a disk-shaped miniature heat pipe with nanofluid," in *Fifth International Conference onElectronic Packaging Technology Proceedings*, pp. 389–391, Shanghai, China, Oct 2003.

[10] H. Alijani, B. Çetin, Y. Akkuş, and Z. Dursunkaya, "Effect of design and operating parameters on the thermal performance of aluminum flat grooved heat pipes," *Applied Thermal Engineering*, vol. 132, pp. 174–187, 2018.

[11] L. M. Poplaski, S. P. Benn, and A. Faghr, "Thermal performance of heat pipes using nanofluids," *International Journal of Heat and Mass Transfer*, vol. 107, pp. 358–371, 2017.

[12] S. Venkatachalapathy, G. Kumaresan, and S. Suresh, "Performance analysis of cylindrical heat pipe using nanofluids - an experimental study," *International Journal of Multiphase Flow*, vol. 72, pp. 188–197, 2015.

[13] K. M. Kim and I. C. Bang, "Effects of graphene oxide nanofluids on heat pipe performance and capillary limits," *International Journal of Thermal Sciences*, vol. 100, pp. 346–356, 2016.

[14] Z. Wan, J. Deng, B. Li, Y. Xu, X. Wang, and Y. Tang, "Thermal performance of a miniature loop heat pipe using water-copper nanofluid," *Applied Thermal Engineering*, vol. 78, pp. 712–719, 2015.

[15] A. B. Solomon, K. Ramachandran, L. G. Asirvatham, and B. C. Pillai, "Numerical analysis of a screen mesh wick heat pipe with Cu/water nanofluid," *International Journal of Heat and Mass Transfer*, vol. 75, pp. 523–533, 2014.

[16] A. Akbari and M. H. Saidi, "Experimental investigation of nanofluid stability on thermal performance and flow regimes in pulsating heat pipe," *Journal of Thermal Analysis and Calorimetry*, vol. 135, no. 3, pp. 1835–1847, 2019.

[17] H. Salehi, S. Zeinali Heris, M. Koolivand Salooki, and S. H. Noei, "Designing a neural network for closed thermosyphon with nanofluid using a genetic algorithm," *Brazilian Journal of Chemical Engineering*, vol. 28, no. 1, pp. 157–168, 2011.

[18] M. Ghanbarpour, N. Nikkam, R. Khodabandeh, and M. S. Toprak, "Improvement of heat transfer characteristics of cylindrical heat pipe by using SiC nanofluids," *Applied Thermal Engineering*, vol. 90, pp. 127–135, 2015.

[19] S. Z. Heris, M. Fallahi, M. Shanbedi, and A. Amiri, "Heat transfer performance of two-phase closed thermosyphon with oxidized CNT/water nanofluids," *Heat and Mass Transfer*, vol. 52, no. 1, pp. 85–93, 2016.

[20] S. Zeinali Heris, M. Shokrgozar, S. Poorpharhang, M. Shanbedi, and S. H. Noie, "Experimental study of heat transfer of a car radiator with CuO/ethylene glycol-water as a coolant," *Journal of Dispersion Science and Technology*, vol. 35, no. 5, pp. 677–684, 2014.

[21] M. F. Nabil, W. H. Azmi, K. Abdul Hamid, R. Mamat, and F. Y. Hagos, "An experimental study on the thermal conductivity and dynamic viscosity of TiO_2-SiO_2 nanofluids in water: ethylene glycol mixture," *International Communications in Heat and Mass Transfer*, vol. 86, pp. 181–189, 2017.

[22] S. Akilu, A. T. Baheta, M. A. M. Said, A. A. Minea, and K. V. Sharma, "Properties of glycerol and ethylene glycol mixture based SiO_2-CuO/C hybrid nanofluid for enhanced solar energy transport," *Solar Energy Mat and Solar Cells*, vol. 179, pp. 118–128, 2018.

[23] T. Yiamsawas, O. Mahian, A. S. Dalkilic, S. Kaewnai, and S. Wongwises, "Experimental studies on the viscosity of TiO_2 and Al_2O_3 nanoparticles suspended in a mixture of ethylene glycol and water for high temperature applications," *Applied Energy*, vol. 111, pp. 40–45, 2013.

[24] M. H. Esfe, S. Wongwises, A. Naderi et al., "Thermal conductivity of Cu/TiO_2-water/EG hybrid nanofluid: experimental data and modeling using artificial neural network and correlation," *International Communications in Heat and Mass Transfer*, vol. 66, pp. 100–104, 2015.

[25] M. Keshavarz Moraveji and S. Razvarz, "Experimental investigation of aluminum oxide nanofluid on heat pipe thermal performance," *International Communications in Heat and Mass Transfer*, vol. 39, no. 9, pp. 1444–1448, 2012.

[26] S. H. Noie, S. Z. Heris, M. Kahani, and S. M. Nowee, "Heat transfer enhancement using Al_2O_3/water nanofluid in a two-phase closed thermosyphon," *International Journal of Heat and Fluid Flow*, vol. 30, no. 4, pp. 700–705, 2009.

[27] M. Ghalambaz, H. Arasteh, R. Mashayekhi, A. Keshmiri, P. Talebizadehsardari, and W. Yaïci, "Investigation of overlapped twisted tapes inserted in a double-pipe heat exchanger using two-phase nanofluid," *Nanomaterials*, vol. 10, no. 9, p. 1656, 2020.

[28] J. S. Lee, Y. M. Seo, C. H. Jeong, M. S. Kim, Y. G. Park, and M. Y. Ha, "Numerical analysis and design optimization of engine room to improve cooling performance for a mid-class excavator," *Journal of Mechanical Science and Technology*, vol. 33, no. 7, pp. 3265–3275, 2019.

[29] A. M. Elsaid, "Experimental study on the heat transfer performance and friction factor characteristics of Co_3O_4 and Al_2O_3 based H_2O/$(CH_2OH)_2$ nanofluids in a vehicle engine radiator," *International Communications in Heat and Mass Transfer*, vol. 108, p. 104263, 2019.

[30] D. Korres, E. Bellos, and C. Tzivanidis, "Investigation of a nanofluid-based compound parabolic trough solar collector under laminar flow conditions," *Applied Thermal Engineering*, vol. 149, pp. 366–376, 2019.

[31] E. Bellos and C. Tzivanidis, "Thermal efficiency enhancement of nanofluid-based parabolic trough collectors," *Journal of Thermal Analysis and Calorimetry*, vol. 135, no. 1, pp. 597–608, 2019.

[32] R. Loni, E. A. Asli-Areh, B. Ghobadian et al., "Research and review study of solar dish concentrators with different nanofluids and different shapes of cavity receiver: experimental tests," *Renewable Energy*, vol. 145, pp. 783–804, 2020.

[33] Z. Said, M. Gupta, H. Hegab et al., "A comprehensive review on minimum quantity lubrication (MQL) in machining

processes using nano-cutting fluids," *International Journal of Advanced Manufacturing Technology*, vol. 105, no. 5-6, pp. 2057–2086, 2019.

[34] Y. Zhou, X. Wu, X. Zhong et al., "Polymer nanoparticles based nano-fluid for enhanced oil recovery at harsh formation conditions," *Fuel*, vol. 267, p. 117251, 2020.

[35] M. Sheikhpour, M. Arabi, A. Kasaeian, A. Rokn Rabei, and Z. Taherian, "Role of nanofluids in drug delivery and biomedical technology: methods and applications," *Nanotechnology, Science and Applications*, vol. Volume 13, pp. 47–59, 2020.

[36] Y. P. Yew, K. Shameli, M. Miyake et al., "Green biosynthesis of superparamagnetic magnetite Fe_3O_4 nanoparticles and biomedical applications in targeted anticancer drug delivery system: a review," *Arabian Journal of Chemistry*, vol. 13, no. 1, pp. 2287–2308, 2020.

[37] A. B. Çolak, "Experimental study for thermal conductivity of water-based zirconium oxide nanofluid: developing optimal artificial neural network and proposing new correlation," *International Journal of Energy Research*, vol. 45, no. 2, pp. 2912–2930, 2021.

[38] M. M. Sarafraz, O. Pourmehran, B. Yang, and M. Arjomandi, "Assessment of the thermal performance of a thermosyphon heat pipe using zirconia-acetone nanofluids," *Renewable Energy*, vol. 136, pp. 884–895, 2019.

[39] M. Sarafraz, T. Kiani, and F. Hormozi, "Critical heat flux and pool boiling heat transfer analysis of synthesized zirconia aqueous nano-fluids," *International Communications in Heat and Mass Transfer*, vol. 70, pp. 75–83, 2016.

[40] M. A. Sharafeldin and G. Grósf, "Experimental investigation of flat plate solar collector using CeO_2-water nanofluid," *Energy Conversion and Management*, vol. 155, pp. 32–41, 2018.

[41] K. S. Suganthi, S. Manikandan, N. Anusha, and K. S. Rajan, "Cerium oxide–ethylene glycol nanofluids with improved transport properties: preparation and elucidation of mechanism," *Journal of the Taiwan Institute of Chemical Engineers*, vol. 49, pp. 183–191, 2014.

[42] M. H. Esfe, F. Zabihi, H. Rostamian, and S. Esfandeh, "Experimental investigation and model development of the non-Newtonian behavior of CuO-MWCNT-10w40 hybrid nanolubricant for lubrication purposes," *Journal of Molecular Liquids*, vol. 249, pp. 677–687, 2018.

[43] M. H. Esfe, K. Motahari, E. Sanatizadeh, M. Afrand, H. Rostamian, and M. R. H. Ahangar, "Estimation of thermal conductivity of CNTs-water in low temperature by artificial neural network and correlation," *International Communications in Heat and Mass Transfer*, vol. 76, pp. 376–381, 2015.

[44] M. H. Esfe, M. Firouzi, H. Rostamian, and M. Afrand, "Prediction and optimization of thermophysical properties of stabilized Al_2O_3/antifreeze nanofluids using response surface methodology," *Journal of Molecular Liquids*, vol. 261, pp. 14–20, 2018.

[45] S. H. Rostamian, M. Biglari, S. Saedodin, and M. Hemmat Esfe, "An inspection of thermal conductivity of CuO-SWCNTs hybrid nanofluid versus temperature and concentration using experimental data, ANN modeling and new correlation," *Journal of Molecular Liquids*, vol. 231, pp. 364–369, 2017.

[46] W. Gao, H. Moayedi, and A. Shahsavar, "The feasibility of genetic programming and ANFIS in prediction energetic performance of a building integrated photovoltaic thermal (BIPVT) system," *Solar Energy*, vol. 183, pp. 293–305, 2019.

[47] A. H. Al-Waeli, K. Sopian, H. A. Kazem et al., "Comparison of prediction methods of PV/T nanofluid and nano-PCM system using a measured dataset and artificial neural network," *Solar Energy*, vol. 162, pp. 378–396, 2018.

[48] M. J. Prakash, V. Sivakumar, K. Thirugnanasambandham, and R. Sridhar, "Artificial neural network and response surface methodology modeling in mass transfer parameters predictions during osmotic dehydration of Carica papaya L," *Alexandria Engineering Journal*, vol. 52, no. 3, pp. 507–516, 2013.

[49] K. N. Shukla, A. Brusly Solomon, B. C. Pillai, B. Jacob Ruba Singh, and S. Saravana Kumar, "Thermal performance of heat pipe with suspended nano-particles," *Heat and Mass Transfer*, vol. 48, no. 11, pp. 1913–1920, 2012.

[50] R. Vidhya, T. Balakrishnan, and B. Suresh Kumar, "Experimental and theoretical investigation of heat transfer characteristics of cylindrical heat pipe using Al_2O_3–SiO_2/W-EG hybrid nanofluids by RSM modeling approach," *Journal of Engineering and Applied Science*, vol. 68, no. 1, pp. 1–20, 2021.

[51] M. Vijayakumar, P. Navaneethakrishnan, and G. Kumaresan, "Thermal characteristics studies on sintered wick heat pipe using CuO and Al_2O_3 nanofluids," *Experimental Thermal and Fluid Science*, vol. 79, pp. 25–35, 2016.

[52] P.-Y. Wang, X.-J. Chen, Z.-H. Liu, and Y.-P. Liu, "Application of nanofluid in an inclined mesh wicked heat pipes," *Thermochimica Acta*, vol. 539, pp. 100–108, 2012.

[53] S. Z. Heris, Z. Edalati, S. H. Noie, and O. Mahian, "Experimental investigation of Al_2O_3/water nanofluid through equilateral triangular duct with constant wall heat flux in laminar flow," *Heat Transfer Engineering*, vol. 35, no. 13, pp. 1173–1182, 2014.

[54] M. H. Esfe and M. H. Hajmohammad, "Thermal conductivity and viscosity optimization of nanodiamond-Co_3O_4/EG (40:60) aqueous nanofluid using NSGA-II coupled with RSM," *Journal of Molecular Liquids*, vol. 238, pp. 545–552, 2017.

[55] M. Hemmat Esfe, A. A. Abbasian Arani, R. Shafiei Badi, and M. Rejvani, "ANN modeling, cost performance and sensitivity analyzing of thermal conductivity of DWCNT–SiO_2/EG hybrid nanofluid for higher heat transfer," *Journal of Thermal Analysis and Calorimetry*, vol. 131, no. 3, pp. 2381–2393, 2018.

[56] M. Shanbedi, S. Z. Heris, A. Maskooki, and H. Eshghi, "Statistical analysis of laminar convective heat transfer of MWCNT-deionized water nanofluid using the response surface methodology," *Numerical Heat Transf. Part A*, vol. 68, no. 4, pp. 454–469, 2015.

[57] A. Afzal, A. M. Samee, and R. A. Razak, "Experimental thermal investigation of CuO-W nanofluid in circular minichannel," *Model Meas Control B*, vol. 86, no. 2, pp. 335–344, 2017.

[58] M. Kumar, A. Afzal, and M. K. Ramis, "Investigation of physicochemical and tribological properties of TiO_2 nano-lubricant oil of different concentrations," *TRIBOLOGIA-Finnish Journal of Tribology*, vol. 35, pp. 6–15, 2017.

[59] A. Afzal, A. D. M. Samee, and R. K. A. Razak, "Comparative thermal performance analysis of water, engine coolant oil and MWCNT-W nanofluid in a radiator," *Model Meas Control B*, vol. 87, no. 1, pp. 1–6, 2018.

[60] A. Afzal, A. D. Mohammed Samee, A. Javad, S. Ahamed Shafvan, P. V. Ajinas, and K. M. Ahammedul Kabeer, "Heat transfer analysis of plain and dimpled tubes with different spacings," *Heat Transfer Researh*, vol. 47, no. 3, pp. 556–568, 2018.

[61] K. M. Yashawantha, A. Asif, G. Ravindra Babu, and M. K. Ramis, "Rheological behavior and thermal conductivity of graphite–ethylene glycol nanofluid," *Journal of Testing and Evaluation*, vol. 49, p. 20190255, 2019.

[62] A. Afzal, S. A. Khan, and C. A. Salee, "Role of ultrasonication duration and surfactant on characteristics of ZnO and CuO nanofluids," *Materials Research Express*, vol. 6, no. 11, p. 1150d8, 2019.

[63] M. E. M. Soudagar, N. N. Nik-Ghazali, M. A. Kalam et al., "The effects of graphene oxide nanoparticle additive stably dispersed in dairy scum oil biodiesel-diesel fuel blend on CI engine: performance, emission and combustion characteristics," *Fuel*, vol. 257, p. 116015, 2019.

[64] A. Afzal, A. D. Mohammed Samee, and R. K. Abdul Razak, "Experimental investigation of thermal performance of engine coolant oil and water in helical coil heat exchanger," *Journal of Engineering Research*, vol. 8, pp. 333–351, 2019.

[65] A. Afzal, I. Nawfal, I. M. Mahbubul, and S. S. Kumbar, "An overview on the effect of ultrasonication duration on different properties of nanofluids," *Journal of Thermal Analysis and Calorimetry*, vol. 135, no. 1, pp. 393–418, 2019.

[66] A. Afzal, A. Aabid, A. Khan et al., "Response surface analysis, clustering, and random forest regression of pressure in suddenly expanded high-speed aerodynamic flows," *Aerospace Science and Technology*, vol. 107, p. 106318, 2020.

[67] M. E. M. Soudagar, A. Afzal, M. R. Safaei et al., "Investigation on the effect of cottonseed oil blended with different percentages of octanol and suspended MWCNT nanoparticles on diesel engine characteristics," *Journal of Thermal Analysis and Calorimetry*, vol. 147, pp. 543–543, 2022.

[68] L. Samylingam, N. Aslfattahi, R. Saidur, S. Mohd, and A. Afzal, "Thermal and energy performance improvement of hybrid PV/T system by using olein palm oil with MXene as a new class of heat transfer fluid," *Solar Energy Materials & Solar Cells*, vol. 218, p. 110754, 2020.

[69] A. Afzal, C. A. Saleel, I. A. Badruddin et al., "Human thermal comfort in passenger vehicles using an organic phase change material-an experimental investigation, neural network modelling, and optimization," *Building and Environment*, vol. 180, p. 107012, 2020.

[70] R. Dhairiyasamy, B. Saleh, M. Govindasamy, A. A. Aly, A. Afzal, and Y. Abdelrhman, "Effect of particle size on thermophysical and heat transfer properties of Ag nanofluid in a radiator–an experimental investigation," *Inorganic and Nano-Metal Chemistry*, pp. 1–15, 2021.

[71] S. Krishnakumar, T. M. Y. Khan, C. R. Rajashekhar, M. E. M. Soudagar, A. Afzal, and A. Elfasakhany, "Influence of graphene nano particles and antioxidants with waste cooking oil biodiesel and diesel blends on engine performance and emissions," *Energies*, vol. 14, no. 14, p. 4306, 2021.

[72] Ü. Ağbulut, S. Sarıdemir, U. Rajak, F. Polat, A. Afzal, and T. N. Verma, "Effects of high-dosage copper oxide nanoparticles addition in diesel fuel on engine characteristics," *Energy*, vol. 229, p. 120611, 2021.

[73] R. Jilte, A. Afzal, M. T. Islam, and A. M. Manokar, "Hybrid cooling of cylindrical battery with liquid channels in phase change material," *International Journal of Energy Research*, vol. 45, no. 7, pp. 11065–11083, 2021.

[74] A. Afzal, K. M. Y. Navid, R. Saidur, R. K. A. Razak, and R. Subbiah, "Back propagation modeling of shear stress and viscosity of aqueous ionic-MXene nanofluids," *Journal of Thermal Analysis and Calorimetry*, vol. 145, no. 4, pp. 2129–2149, 2021.

[75] R. Jilte, A. Afzal, and S. Panchal, "A novel battery thermal management system using nano-enhanced phase change materials," *Energy*, vol. 219, p. 119564, 2021.

[76] B. V. Chaluvaraju, A. Afzal, D. A. Vinnik, A. R. Kaladgi, S. Alamri, and V. Tirth, "Mechanical and corrosion studies of friction stir welded nano Al_2O_3 reinforced Al-Mg matrix composites: RSM-ANN modelling approach," *Symmetry (Basel)*, vol. 13, no. 4, p. 537, 2021.